

# THE X1 CATALOGUE OF POSITIONS AND PROPER MOTIONS OF FAINT STARS AROUND THE ICRF SOURCES

P. N. Fedorov, A. A. Myznikov

*Institute of Astronomy, V. N. Karazin Kharkiv National University  
35 Sumska Str., 61022 Kharkiv, Ukraine  
e-mail: pnf@astron.kharkov.ua, myznikov@astron.kharkov.ua*

---

We present a new catalogue of faint astrometric reference stars around ICRF sources of northern hemisphere. The X1 catalogue is obtained at the Institute of Astronomy of the V.N. Karazin Kharkiv National University and contains about 1.3 million positions and proper motions of stars from  $10^m$  to  $19^m$  within  $330\ 1^\circ \times 1^\circ$  fields. Mean positions and proper motions of stars were derived from reprocessing and astrometric reduction of digitized images of Schmidt plates POSS-I and POSS-II sky surveys obtained from USNOFS PMM Image Archive. The Tycho-2 stars were used as reference stars. The mean errors of the positions at mean epoch are 50 to 100 mas, depending on magnitude and particular field. Proper motions errors are about 2.5 to 5 mas/yr depending on magnitude. Estimated external errors are close to internal errors mentioned. The source data, brief outlines of the image processing and reduction techniques, main features of the catalogue, as well as some results of external comparisons are presented.

---

## INTRODUCTION

As it is known, rigorous solution of problem of relationship between optical (Hipparcos) and radio (ICRF) coordinate systems implies the knowledge of accurate positions of the main reference points in both these systems. The link between these systems was established by variety of methods (Kovalevsky *et al.* [2]). The alignment of both systems at the Hipparcos mean epoch was established with an uncertainty of 0.6 mas and 0.25 mas/yr in the position and global rotation of zero points, respectively. Among variety of used data, only 78 optical counterparts of extragalactic radio sources were used for this solution.

The test of this link was carried out by N. Zacharias [12] using 327 optical positions of ICRF sources. However, this test could not be strict, despite applying the kinematic corrections, through lack of knowledge of proper motions of reference stars. For strict solution of the link problem the densification of the Hipparcos system, expansion of it to faint stars and obtaining of proper motions of stars are necessary.

The goal of this work is deriving of positions and proper motions of stars in areas of sky around the ICRF sources of northern hemisphere. This work was fulfilled by reprocessing and reduction of digitized images of the Palomar Observatory Sky Surveys POSS-I and POSS-II plates. Big enough epoch difference between these surveys allow us to expect obtaining of accurate proper motions of stars.

As it is well known, astrometry of Schmidt plates is very difficult through pattern of systematic deformations that appear in them. These difficulties seem formidable for areas about  $6^\circ \times 6^\circ$  of size, but we overcame most of these difficulties for small fields sized about  $1^\circ \times 1^\circ$ .

Here we present the X1 catalogue of position and proper motions of faint stars around 330 northern hemisphere ICRF sources, briefly describe the image processing and reduction techniques, as well as bring the main features of catalogue. Additionally, we bring main results of external comparisons of X1 positions and proper motions.

Using positions of 190 optical counterparts of ICRF sources, found among X1 stars, for the first time was done the strict solution of problem of link between Hipparcos and ICRF. Obtained values of orientation angles and their time variations indicate the good quality of X1 both in random and systematic respects.

## INDIVIDUAL POSITIONS

### *Source data*

The X1 catalogue is based on the Palomar Observatory Sky Surveys POSS-I (Minkowski & Abel 1963) and POSS-II (Reid *et al.* [7]). These surveys were carried out using the Palomar Observatory 48-inch Oschin Schmidt

telescope in 1949–1958 (POSS-I) and in the 1980s–1990s (POSS-II). Because of big enough epoch difference between these surveys, it was expected to derive the accurate proper motions.

The digitized images of POSS-I O, E and POSS-II N, F, and J plates produced by USNO Flagstaff Station Precision Measuring Machine (PMM) were obtained from USNOFS PMM Image Archive and used for creating the catalogue. The PMM images are acquired and digitized by two CCD cameras with a useful area of  $1312 \times 1033$  pixels. The pixels are squares of 6.8 microns on a side, have no dead space between pixels (100% filling factor), and there are no bad pixels in the array (Class 0). Printing–Nikkor lenses were used for projection to CCD chip the plate areas  $\approx 18 \times 14 \text{ mm}^2$  of size with scale about of  $\approx 13.7 \text{ mkm}$  per pixel ( $\approx \times 0.9 \text{ arcsec/pixel}$  of sky scale). The individual PMM scans are uniformly quantized on 256 intensity levels and saved in FITS files. Each individual PMM scan covered the sky area about of  $\approx 19' \times 15'$  size and contains from a few hundreds to few thousands of star images.

Traditional methods were used to preprocess individual PMM images – the flat field processing, image filtration, estimation of background level and its dispersion, *etc.* Then, special software created in astrometry department of the Institute of Astronomy of the V. N. Karazin Kharkiv National University was employed to detect and analyze of separate images of stars on individual PMM scans. Bad images (rubbish on photoemulsion, overlapped images of stars, images of galaxies with perceptible structure) were rejected and excluded from further processing.

The quality of star images was found to vary depending on magnitude and distance to plate center. While faint stars have relatively symmetric bell-shaped circular image profile, images of brighter stars are very oversaturated and are asymmetrical when lie away from plate center.

The two-dimensional circular exponential model was used to fit the accurate image profiles:

$$I(x, y) = A \cdot \exp(-|r|^4), \quad r = \sqrt{(x - x_0)^2 + (y - y_0)^2}. \quad (1)$$

This model gave relatively stable results both for faint and bright stars, even for very saturated and strained images.

Since oversaturation the images of stars brighter than about  $9^m$ – $10^m$  magnitude are very difficult to measure, and their measured positions may differ from the correct position by more than the few hundred mas. This effect is especially large near the plate edges. In fact, only stars fainter than about 10th magnitude were more or less successfully measured and passed in further processing. The accuracy of measurement of their coordinates depends from magnitude, plate type, emulsion grain, distance to plate center, as well as from the quality of particular image. The accuracy of measurement was found about of 0.8 microns for good, relatively faint images, and to few microns for the brightest and very faint stars.

Thus, although Tycho-2 positions and proper motions of brightest stars are very accurate, only subset of Tycho-2 stars from about  $10^m$  to  $12^m$  magnitude range was used as reference.

### ***Mosaics***

Individual PMM scans have relatively small size on the celestial sphere ( $\approx 15' \times 19'$ ), and, therefore, number of reference Tycho-2 stars on the one PMM scan is not enough to make astrometry.

In order to cover one square degree area of sky, the lists of detected stars from individual PMM scans were gathered into one common list of stars. This list, so-called “mosaic”, covers plate area about 5 cm of size and contains about 1 to 20 thousands of stars.

The measured scan coordinates of stars were converted into corresponding plate coordinates using information from special sensors of PMM machine. Conceptually, data from these sensors allow to convert coordinates of any point at particular scan into corresponding plate coordinates. Unfortunately, values of PMM sensors were found to be not enough accurate, and moreover, sometimes incorrect. For creating a mosaic correctly, we created and applied the empirical algorithms, which used overlap zones of adjacent scans. These overlap zones, about 2 mm wide, usually contains several tens of star images common for pair of adjacent scans. Using of this information has allowed to correct, to some degree, values of PMM sensors.

Result of this stage was the list of all stars, detected on one square degree field, with information about their measured plate coordinates, fluxes and other characteristics.

### ***Plate reduction***

Base idea is that field size of  $1^\circ \times 1^\circ$  is relatively small area of Schmidt plate, and therefore, the plate model in such small region can be close to flat. This idea was discussed in details by Taff in [9, 10].

For each mosaic the Tycho-2 stars were selected from catalogue and its apparent places at epoch of the observation were computed. Individual Tycho-2 stars were identified with corresponding entries in detection list and were used as reference stars. Because of difficulties to measure positions of bright stars, only Tycho-2 stars with  $B_T \gtrsim 9.5^m$  for blue plates and  $V_T \gtrsim 9.5^m$  for red plates were used. The most frequent number of

reference stars was about 25–30 per field. If number of reference stars on particular mosaic was less than 15 then reduction was not made and this mosaic was excluded from processing.

We explored and tested several reduction models. It was found that use of simple linear model with preliminary excluding nominal cubic distortion of Schmidt telescope is insufficient to making the reduction at 0.1 arcsec level. Remaining residuals of reduction were sufficiently big. More complex nonlinear reduction models not gave a stable results because of relatively small number of reference Tycho-2 stars per field and not enough accuracy of their catalogue and measured positions.

Analysis of nonlinear geometric distortions was made using following reduction model for each mosaic:

$$\begin{cases} x = a_{0,0} + a_{0,1} \cdot \xi + a_{0,2} \cdot \eta + a_{0,3} \cdot \xi \cdot \eta + a_{0,4} \cdot \eta^2, \\ y = a_{1,0} + a_{1,1} \cdot \xi + a_{1,2} \cdot \eta + a_{1,3} \cdot \xi \cdot \eta + a_{1,4} \cdot \xi^2. \end{cases} \quad (2)$$

Optical centre was accepted to be in the geometric centre of particular field.

By solving of these conditional equations, the coefficients at nonlinear terms were calculated for each particular mosaic. After processing by such manner of the whole available data (more than 400 mosaics on each of five plate types), all calculated coefficients were gathered and analyzed for the dependence from plate type and from the position of field over the plate. As a result, the distributions of these coefficients over plate were fitted as a relative simple functions of plate coordinates. Then, measured coordinates of all stars were corrected using these approximations. When correction of measured coordinates for nonlinear distortions was made, usual linear reduction was used and its residuals were analyzed for dependence on magnitude.

Making the accurate photometry was not issued in this work. However, to correct magnitude equation, it was necessary to obtain approximate magnitudes of stars. USNO-A2.0 red and blue magnitudes were adopted as a reference to derive our own magnitudes from measured fluxes of star images. Authors understand that it is not the best method for deriving of magnitudes, but on some reasons it was adopted. Since the each star was measured on several plates, the final X1 magnitude was derived by averaging of the individual red magnitudes obtained from POSS-I E and POSS-II F plates. In general, the final X1 magnitudes are roughly by  $0.5^m$  to  $1^m$  brighter than UCAC2 ones at  $11^m$ – $16^m$  magnitude range, are very crude, and can be used only for identification purposes.

The magnitude equation was obtained from the analysis of dependence of reduction residuals on measured magnitudes of stars. It was found that the magnitude equation depends on plate type and for each plate type may be satisfactorily expressed as a sum of two additive terms – linear shift of star coordinates proportionately to star magnitude, and radial shift, depended on magnitude and distance to plate center.

Linear part of magnitude equation was computed on the assumption, that mean value of radial pattern is equal to zero. After subtraction of it, remaining magnitude equation was considered as clearly radial pattern. To analyze it in all magnitude range the data from catalogues M2000 (Rapaport *et al.* [6]), UCAC2 (Zacharias *et al.*, [13]) ( $10^m$ – $16^m$ ), ACR (Stone *et al.* [8]) ( $10^m$ – $18^m$ ), as well as coordinates of some faint galaxies and quasars were used in addition to Tycho-2. These data cover only some areas of sky, but contains high-accuracy positions of stars fainter than the Tycho-2 catalogue. As a result, the radial pattern was fitted as a function of magnitude and distance from plate center. Then, the measured coordinates of all stars were corrected for this magnitude pattern.

After correction for magnitude equation and non-linear distortions terms, usual linear reduction was used for each mosaic. The mean value of weight unit error was found about 140 and 120 mas for plates of POSS-I and POSS-II, respectively. For each field 5 up to 10 plates taken at different epochs from 1949 to 1999 were available. As the result, for each field was obtained the set of individual catalogues of star positions at particular epochs.

## MEAN POSITIONS AND PROPER MOTIONS

Mean positions and proper motions of stars were derived from their individual positions at particular epochs. Only stars successfully measured on the all plates of particular field were used. To derive the mean positions and proper motions of stars from their individual positions at individual epochs  $t_i$ , the linear regression was used:

$$x(t_i) = x_0 + \mu_x \cdot (t_i - t_0), \quad (3)$$

where  $x$  means right ascension (or declination),  $t_0$  is mean epoch of the observations. No weighing was applied. For each star the standard errors of the position and proper motions were computed from scatter of regression residuals:

$$\sigma_x^2 = \frac{\sum (x_i - x_0)^2}{n \cdot (n - 2)}, \quad \sigma_{\mu_x}^2 = \frac{\sum (x_i - x_0)^2}{(n - 2) \cdot \sum (t_i - t_0)^2}, \quad (4)$$

where  $n$  is the number of star observations, and  $x_i$  is the individual star position at epoch  $t_i$ . For stars with six or more individual positions, the several statistics were used to determine which observations are outliers. All outliers were removed and regression was repeated.

As it is known, the scatter of regression residuals can give an erroneous value of standard error when number of used observations is not large. Therefore, another technique was employed to determine more realistic estimations of X1 internal errors. For each individual catalogue we previously estimated the errors of catalogue positions  $\sigma_{x_i}$  depending on magnitude. Then, using these predetermined values, for each star the mean formal errors were computed:

$$\sigma_x^2 = \frac{\sum \sigma_{x_i}^2}{n^2}, \quad \sigma_{\mu x}^2 = \frac{\sum \sigma_{x_i}^2}{n \cdot \sum (t_i - t_0)^2}. \quad (5)$$

After processing of the whole data set, all formal errors were collected in 1.0 magnitude bins from  $9^m$  to  $19^m$  and the mean values were computed for each bin.

The mean errors were found about 50 to 100 mas and 2.5 to 5 mas/yr in position and proper motion, respectively, depending on magnitude (see Fig. 1). The average value of mean epochs is about of 1978. Since the different number of plates was available for each field, as well as due to the center of each field was referred to the various sites at different photoplates, we suppose that the real errors of positions and proper motions may vary from field to field.

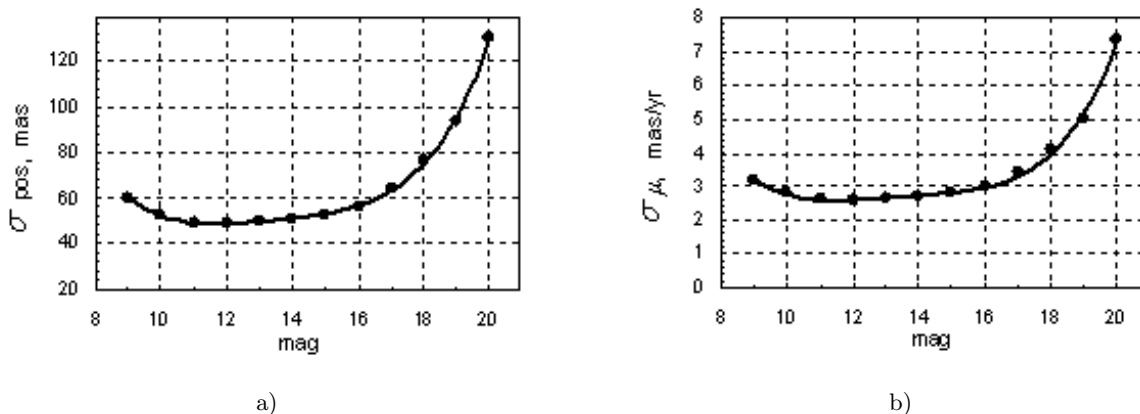


Figure 1. The mean, formal errors of X1 positions (a) at mean epoch and proper motions (b) as function of X1 magnitude

## EXTERNAL COMPARISONS

### *Comparisons with the UCAC2, 2MASS, and ERLCat*

In order to estimate the X1 external errors, various external comparisons were performed. The paper with details of these comparisons is in preparation. Here we bring the main results of comparisons with the UCAC2 (Zacharias *et al.* [13]), 2MASS (Curti *et al.*, 2003), and ERLCat data (de Vegt *et al.* [11]).

The 2MASS and ERLCat are not provided the proper motions, so X1 positions were brought to their epochs, using X1 proper motions. Then, the position differences for stars common in X1 and 2MASS, as well as X1 and ERLCat, were computed and analysed.

In general, these comparisons showed that the observed scatter of position differences agrees with expected from the combination of formal internal errors. The systematic position differences for stars common from X1 and 2MASS, as well as X1 and UCAC2, are less than 10–12 mas at epoch close to J2000. The root-mean-squares of random differences are close to 100 mas for stars in  $11^m$ – $16^m$  magnitude range and agree with combination of internal errors of compared catalogues.

The UCAC2 provided the proper motions, so they were used to estimate of external precision of X1 proper motions. Figure 2a shows the systematic differences between X1 and UCAC2 proper motions, as a function of X1 magnitude. As seen, these differences are magnitude depended but not exceed 1.3 mas/yr. The root-mean-squared values of random differences (after subtraction of the systematic part) are showed in Fig. 2b as a function of X1 magnitude.

In bright part (to  $11.5^m$  X1 magnitude) the errors of UCAC2 proper motions are about 1 mas/yr, revealing an external random errors of X1 proper motions less than 3 mas/yr. In the faint part to 16th magnitude the UCAC2 errors dominate over X1 errors [14]. Results of this comparisons not conflict with this fact.

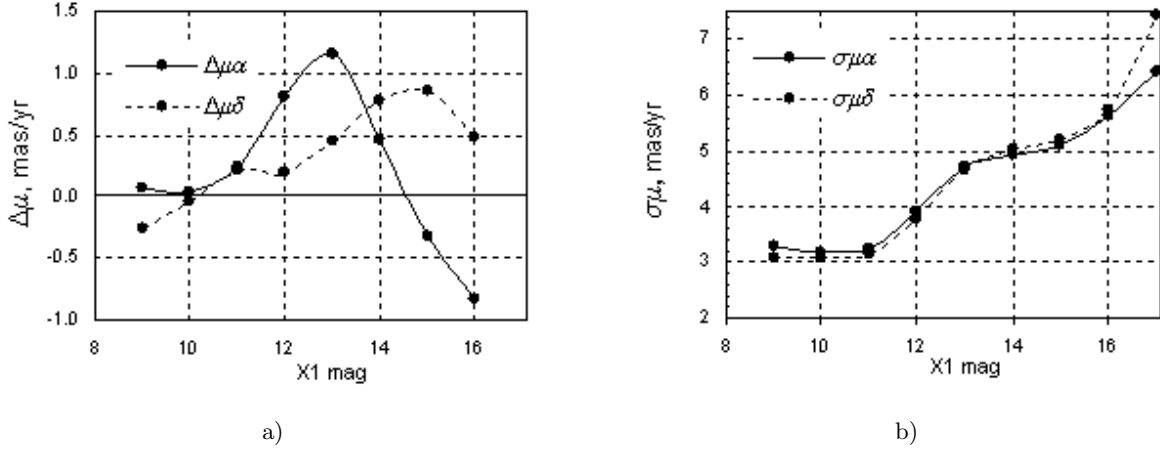


Figure 2. Systematic differences (a) and the root-mean-squares of random differences (b) between X1 and UCAC2 proper motions as function of X1 magnitude

### Non-stellar sources

The X1 contains some galaxies and quasars from ICRF list. The 198 optical counterparts of ICRF sources were found among X1 stars. The optical minus radio position differences were formed and 8 outliers were removed. The rest 190 counterparts were used to estimate external random and systematic errors of X1 catalogue.

Figure 3a shows the distributions of optical minus radio position differences at mean epochs of observation of these objects. The mean value of this distribution is close to vanished for both right ascension and declination; the root-mean-squared deviation is  $\sigma_{O-R} \approx 64$  mas.

Figure 3b shows the distribution of formal proper motions of these objects. This distribution is close to normal with standard deviation  $\sigma_\mu \approx 3.4$  mas/yr.

The corresponding average internal errors for used objects are about 67 mas in position and about 3.6 mas/yr in proper motions, respectively. We suggest that these values agree quite well with the observed scatter of residuals and even are somewhat overestimated.

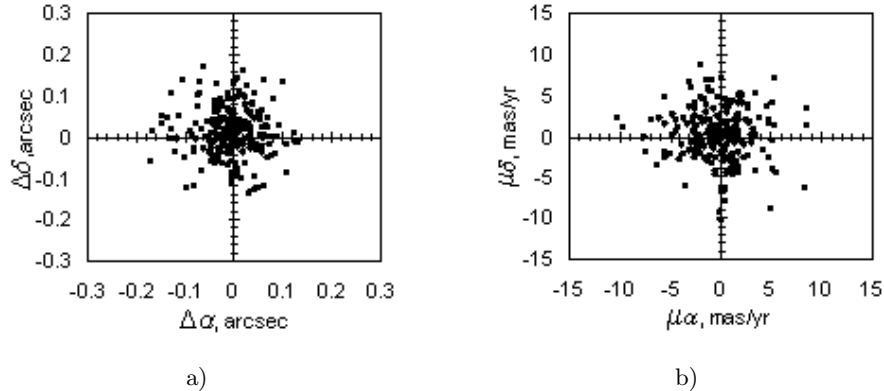


Figure 3. Distribution of the optical minus radio position differences (a) and formal proper motions (b) of the 190 optical counterparts of ICRF sources which found among X1 stars

Also, the optical minus radio differences and formal proper motions of mentioned optical counterparts were used to find orientation and spin between X1 and ICRF, using model of Lindegren & Kovalevsky (1995). The results are showed in Table 1. As seen from the table, the orientation and spin between X1 and ICRF are zeros at given precision. We suggest that these results indicate that no significant errors both in X1 positions and proper motions presented.

Table 1. Elements of orientation and spin between X1 and ICRF

$N$	$\sigma_x$ mas	$\varepsilon_x$ mas	$\varepsilon_y$ mas	$\varepsilon_z$ mas	$\sigma_\mu$ mas/yr	$\omega_x$ mas/yr	$\omega_y$ mas/yr	$\omega_z$ mas/yr
190	63	$+4 \pm 6$	$0 \pm 6$	$-8 \pm 6$	3.3	$-0.26 \pm 0.30$	$-0.34 \pm 0.29$	$-0.25 \pm 0.21$

## RESULTS

The X1 provides reference system with high-accuracy proper motions of stars up to  $19^m$  within areas  $1^\circ \times 1^\circ$  size around ICRF sources of northern hemisphere. At present time X1 contains about 1.3 million stars and provides the density about of 4000 stars per square degree. This allows us to observe ICRF sources using even small CCD-receivers. The internal X1 errors at mean epoch are 50 to 100 mas for positions and 2.5 to 5 mas/yr for proper motions, depending on magnitude and particular field. To easy of use the catalogue, all positions are given at epoch J2000. For each star the mean epoch of observation and formal errors of position and proper motion are given.

The external comparisons show that X1 well extends the Tycho-2 system to faint stars up to  $19^m$ . Obtained elements of orientation indicate both the high quality of X1 catalogue and lack of its considerable degradation with time.

**Acknowledgements.** This work was made use of the USNOFS Image and catalogue Archive operated by the United States Naval Observatory, Flagstaff Station [<http://www.nofs.navy.mil/data/fchpix>]. We are very grateful to Dr. Stephen Levine from USNO Flagstaff Station for the grant of CD's with digitized PMM images of POSS plates.

- [1] *Harrington R. G.* The 48-inch Schmidt-type telescope at Palomar Observatory // *Publs Astron. Soc. Pacif.*–1952.–**64**.–P. 275.
- [2] *Kovalevsky J. et al.* // *Astron. and Astrophys.*–1997.–**354**.–P. 732.
- [3] *Lund J. M., Dixon R. S.* A user's guide to the Palomar Sky Survey // *Publs Astron. Soc. Pacif.*–1973.–**85**.–P. 230.
- [4] *Mignard F.* Report of the IAU Working Group on ICRS.–2000.
- [5] *Minkowski R., Baade W.* // *Astrophys. J.*–1954.–**119**.P. 206.
- [6] *Rapaport M. et al.* // *Astron. and Astrophys.*–2001.–**376**.–P. 325.
- [7] *Reid I. N. et al.* The Second Palomar Sky Survey // *Publs Astron. Soc. Pacif.*–1991.–**103**.–P. 661.
- [8] *Stone R. C., Pier J. R., Monet D. G.* Improved astrometric calibration regions along the celestial equator // *Astron. J.*–1999.–**118**.–P. 2488.
- [9] *Taff L. G.* Schmidt plate astrometry: subplate overlap // *Astron. J.*–1989.–**98**.–P. 1912.
- [10] *Taff L. G., Lattanzi M. G., Bucciarelli B.* Two successful techniques for Schmidt plate astrometry // *Astrophys. J.*–1990.–**358**.–P. 359.
- [11] *De Vegt C. et al.* // *Astron. J.*–2001.–**121**.–P. 2815.
- [12] *Zacharias N. et al.* // *Astron. J.*–1999.–**118**.–P. 2511.
- [13] *Zacharias N., Urban S. E., Zacharias M. I., et al.* The Second U.S. Naval Observatory CCD Astrograph Catalog (UCAC2) // *Astron. J.*–2004.–**127**.–P. 3043.
- [14] *Zacharias N., Urban S. E., Zacharias M. I., et al.* // *Astron. J.*–2004.–**127**.–P. 3043–3045.